High Sensitive NDE of Subsurface Local Damages in Thermal Barrier Coating Systems by the Laser Speckle Method†

WAKI Hiroyuki*, NISHIKAWA Izuru and KOBAYASHI Akira*****

Abstract

Thermal barrier coatings (TBCs) have been used for insulating a substrate from high temperature in gas turbine plants. High temperature fatigue strength has been an important problem for these components. However, nondestructive evaluation (NDE) of subsurface delamination for a thermal-barrier-coated material has been so difficult that the effect of delamination on the fatigue fracture life of a substrate hasn't been well studied. The relationship between surface strain behavior and the state of any subsurface delamination for a TBC material is described in this paper. Tension-compression fatigue tests were carried out at 873K and room temperature for ZrO_2-$8Y_2O_3$-sprayed and Al_2O_3-sprayed specimens. Surface strain behavior during the fatigue test was measured using the laser speckle method. It was found that surface strain was fully reflected by substrate strain unless subsurface delamination was initiated, while surface strain was found to decrease when subsurface delamination was initiated. All the surface strain behaviors were classified in five patterns, and they were related to the state of subsurface delamination. It was concluded that the surface strain beside a crack was sensitive to the subsurface damage and applicable for evaluating subsurface damage.

KEY WORDS: (NDE) (Thermal Barrier Coating) (Delamination) (Fatigue) (Plasma Spraying) (Surface Strain) (Laser Speckle).

1. Introduction

Thermal barrier coatings (TBCs) have been used for insulating a substrate from high temperature in gas turbine plants[1]. High temperature fatigue strength has been an important problem for these components. However, nondestructive evaluation (NDE) of subsurface delamination for a thermal-barrier-coated material has been so difficult that the effect of delamination on the fatigue fracture life of a substrate hasn't been well studied.

There are some studies[2-4] about surface strain behavior of thermal barrier coated materials, and the authors have developed the laser speckle strain measurement method[5,6]. The method is applicable to local high temperature strain measurement with a good strain resolution. In this study, the method was applied to the NDE of subsurface damage in TBC materials. Fatigue tests were carried out at 873K and room temperature (R.T.) for ZrO_2-$8Y_2O_3$-sprayed and Al_2O_3-sprayed specimens. The relationship between surface strain behavior and the state of subsurface delamination for a thermal-barrier-coated material was examined and compared with the results of a microscopic observation of the specimen. All the surface strain behaviors were classified in five patterns. These strain patterns, which corresponded to delamination patterns, were related to a test temperature and an applied strain level.

2. Experimental Procedure

2.1 Specimen

An hour-glass-shaped specimen was used for the fatigue testing. The shape and dimensions of the substrate are shown in **Fig. 1**. Type 304 stainless steel was used for the substrate. The substrate was shot blasted before spraying. An alloy bond-coating and a ceramic top-coating were deposited on the hatched area in Fig.1. Ceramic coating was deposited by atmospheric plasma spraying (APS). Bond coating was deposited by either APS or low pressure plasma spraying (LPPS). Both spraying powders and spraying conditions are listed in **Table 1** and **Table 2**, respectively. The thicknesses of the bond-coating and the ceramic coating were about 150 μm and 300 μm, respectively. Four types of TBC specimens shown in **Table 3** were manufactured in order to compare the delamination processes. The diffusion thermal treatment in Table 3 was carried out by heating for 3 hours at 1323K in vacuum followed by furnace cooling. The tensile strengths[7], σ_B, and the tensile adhesive strengths, σ_{IF}, of bond-coatings and ceramic-coatings for these four specimens are shown in **Table 4**.

† Received on June 22, 2007
* Osaka Electro-Communication University
** Osaka Institute of Technology
*** Associate Professor

Transactions of JWRI is published by Joining and Welding Research Institute, Osaka University, Ibaraki, Osaka 567-0047, Japan

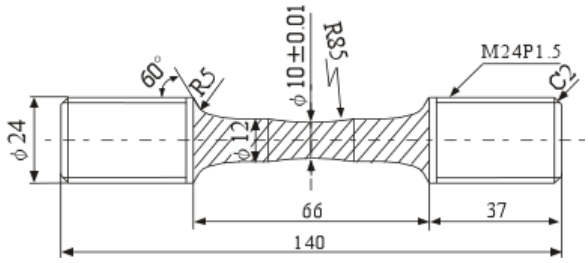

Fig.1 Shape and dimensions of the substrate used in this study.

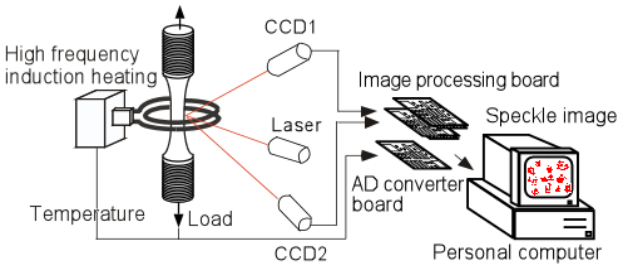

Fig.2 Schematic illustration of the speckle strain measurement system.

Table 1 Spraying powders used in this study.

	ZrO_2-8% Y_2O_3	Al_2O_3	CoNiCrAlY	NiCr
Chemical composition (mass%)	ZrO_2, 8% Y_2O_3	98%Al_2O_3	Co, 32%Ni, 21%Cr, 8%Al, 0.5%Y	Ni, 20%Cr
Powder size (μm)	45~75	15~45	5~37	45~106

Table 2 Plasma-spraying conditions.

		APS metal coating	APS ceramic coating	LPPS metal coating
Pressure (MPa)		0.1	0.1	0.013
Arc current (A)		500	850	500
Arc voltage (V)		60	35	60
Arc gas	Ar (MPa)	0.69	0.41	0.69
	He (MPa)	—	0.62	—
	H_2 (MPa)	0.41	—	0.48
Spraying distance (mm)		150	100	360

Table 3 Four types of thermal-barrier-coated specimens used in this study.

Specimen	Ceramic c.	Bond c.
A-1	Al_2O_3(APS)	NiCr(APS)
Z-1	ZrO_2-8Y_2O_3(APS)	CoNiCrAlY(APS)
Z-2	ZrO_2-8Y_2O_3(APS)	CoNiCrAlY(LPPS)
Z-3	ZrO_2-8Y_2O_3(APS)	CoNiCrAlY(LPPS) with thermal treatment

Table 4 Tensile strengths, σ_B, and tensile adhesive strengths, σ_{IF} for each coating (MPa).

Specimen	Ceramic c.		Bond c.	
	σ_B	σ_{IF}	σ_B	σ_{IF}
A-1	30	10	30	30
Z-1	<30	10	120	>30
Z-2	<30	10	>200	<30
Z-3	<30	10	>200	>30

Table 5 Temperatures of a substrate and a surface under each heating condition.

	Surface temperature (K)	Substrate temperature (K)
Induction heating	873	893
Furnace heating	893	833

2.2 Test procedure

An electro-hydraulic-servo fatigue test machine (max. load=100kN) was used for tension-compression fatigue testing. The fatigue tests were carried out at high temperatures and room temperature with a frequency of 10 Hz, a stress ratio of R= -1 and a constant nominal stress range, $\Delta\sigma_n$. The specimens were heated by either induction heating or furnace heating. The temperatures of the substrate and the surface under each heating condition are shown in **Table 5**. The surface strain behavior during the fatigue test was measured using the laser speckle strain gauge[5,6].

Next, the experimental setup of the laser speckle strain gauge is briefly described. A He-Ne Laser (wave length=682.8 nm, power = 5 mW, spot size diameter =1.0 mm) was used in this study. As a measured strain is known to be an average of this area, the gauge length for the strain measurement is 1.0 mm. Speckle images were taken using a CCD camera with 410 thousand pixels. The CCD angle, θ, and the CCD distance, L, were selected as θ = 30 degrees and L = 163 mm, respectively. When the surface resolution is assumed to be one pixel size which is 5.7 μm, the strain resolution can be calculated as 0.061 % strain. The speckle image signals were introduced into a personal computer through an image processing board with 640 pixel × 485 pixel × 8 bit memories. The schematic illustration of the experimental setup is shown in **Fig.2**. Air turbulence causes an error in the strain measurement at elevated temperature. In order to reduce the convection of hot air, the specimen was placed in a small box. The air turbulence error decreased to less than 0.1% strain at 893K by the introduction of this box.

3. Experimental Results and Discussions

In this chapter, all the measured surface strain behaviors are classified in five patterns. The relationships between the surface strain pattern and the state of subsurface delamination were examined. Surface strain was measured with a gauge length of 1 mm at a distance of 1 mm from a surface crack.

3.1 Nondelamination, pattern (A)

The relationship between nominal stress and surface strain under a low stress range condition at high temperature for an A-1 specimen is shown in **Fig.3**. Surface cracks were initiated immediately after loading. The surface strain gradually decreases with increasing the number of cycles as shown in Fig.3. **Figure 4** shows the comparison of the surface strain range of the A-1 specimen and that of a non-coated specimen with only blast treatment called a substrate specimen. The surface strain of the A-1 specimen is reflected by the substrate strain as shown in Fig.4. A subsurface delamination was not detected by the observation of the longitudinal section of the A-1 specimen after the fatigue testing. The surface strain of a thermal-barrier-coated specimen was found to be reflected by substrate strain when subsurface delamination wasn't initiated even if cracks in the coatings were initiated. The damage model of the coating is illustrated in **Fig.5**. This strain behavior without a delamination is called pattern (A).

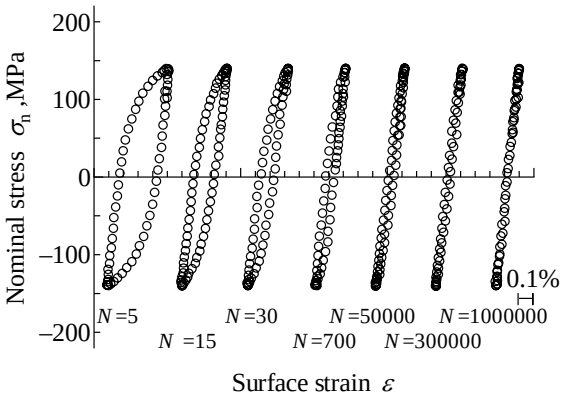

Fig.3 Stress-strain hysteresis loops under $\Delta\sigma_n$=280MPa at 893K for an A-1 specimen (N_f>1000000).

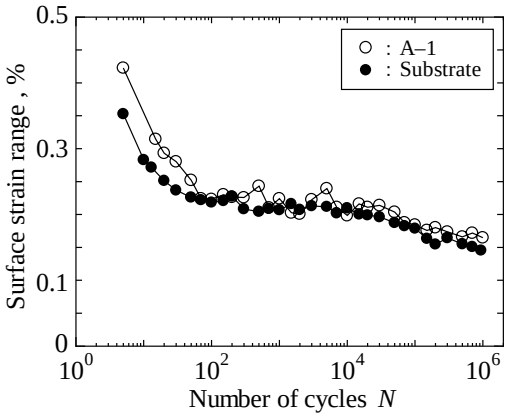

Fig.4 Comparison of the strain behavior of an A-1 specimen and that of a substrate specimen under $\Delta\sigma_n$=280MPa at 893K (N_f>1000000).

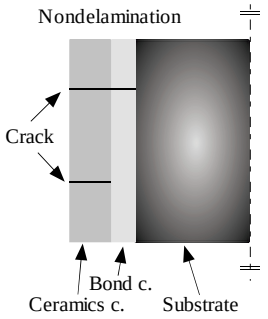

Fig.5 Damage of the coating in pattern (A).

3.2 Delamination growing gradually with crack opening and closure, pattern (B)

The relationship between nominal stress and surface strain under a high stress range condition at R.T. for an A-1 specimen is shown in **Fig.6**. The stress-strain curves of a substrate specimen are also drawn in Fig.6. The substrate specimen shows cyclic softening behavior, however the A-1 specimen shows characteristic strain behavior. The strain of the A-1 specimen decreases at the tension side of a strain. At N=1500 cycles, for example, the surface strain disappears when the nominal stress, $\Delta\sigma_n$, reaches about 175MPa, and the surface strain appears again when $\Delta\sigma_n$ reaches about −200MPa. This characteristic strain behavior resulted from a crack and a small scale delamination whose size was less than 1.5 mm distance from the crack. The damage process of the coating is illustrated in **Fig.7**. In this case, the surface strain near a surface crack with subsurface delamination disappeared during the crack opening period, and the surface strain appeared again when the crack closed. Figure 6 also indicates that the surface crack opening stress decreases with an increase in the number of cycles, and that the crack closure compressive stress increases with an increase in the number of cycles. As the coating has been known to shrink by compressive loading[7-9], the surface crack opening quantity at zero stress increased

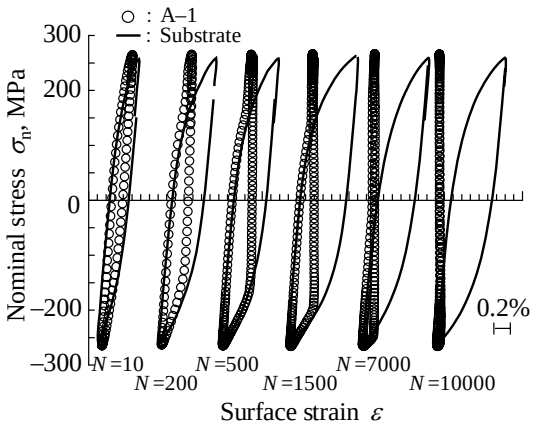

Fig.6 Comparison of the stress-strain hysteresis loops of an A-1 (N_f=10600) specimen and that of a substrate specimen under $\Delta\sigma_n$=530MPa at R.T.

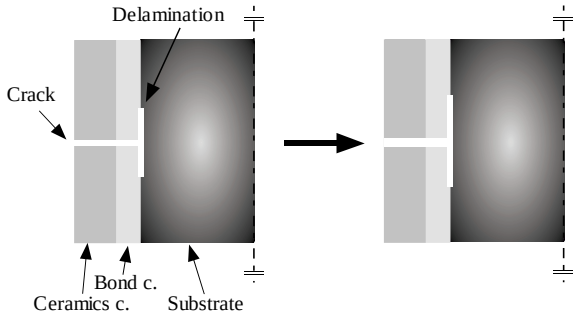

Fig.7 Damage process of the coating in pattern (B).

with an increase in the number of cycles. Therefore, both the surface crack opening stress and the closure stress was transferred as shown in Fig.6. This strain behavior with a small scale delamination is called pattern (B).

3.3 Delamination growing gradually without crack opening and closure, pattern (C)

The relationship between nominal stress and surface strain under a high stress range condition at high temperature for an A-1 specimen is shown in **Fig.8**. The surface strain gradually decreases to zero with an increase in the number of cycles. The comparison of the surface strain range of the A-1 specimen and that of a substrate specimen is shown in **Fig.9**. The surface strain gradually decreases to zero, though the substrate strain appears more than 0.3% throughout the fatigue test as shown in Fig.9. The delamination between a substrate and a bond coating whose size was more than 1.5 mm distance from a surface crack was detected by the observation of the longitudinal section of the specimen after the fatigue test. The damage process of the coating is illustrated in **Fig.10**. A surface strain was found to decrease gradually to zero with an increase in the number of cycles if the subsurface delamination area increased. This strain behavior with a relatively large delamination is called pattern (C).

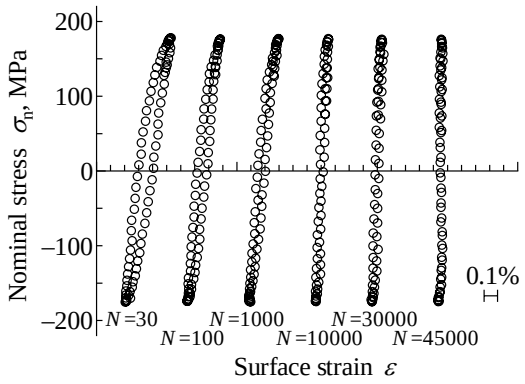

Fig.8 Stress-strain hysteresis loops under $\Delta\sigma_n$=350MPa at 893K for an A-1 specimen (N_f=17750).

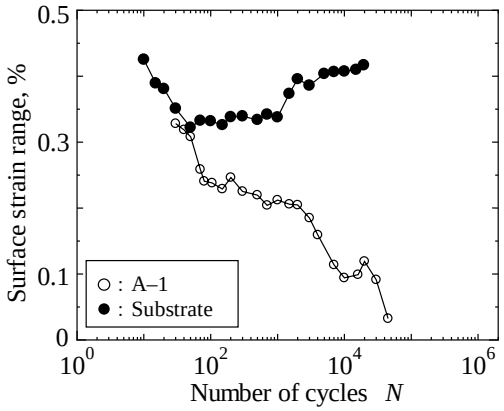

Fig.9 Comparison of the strain behavior of an A-1 specimen and that of a substrate specimen under $\Delta\sigma_n$=350MPa at 893K.

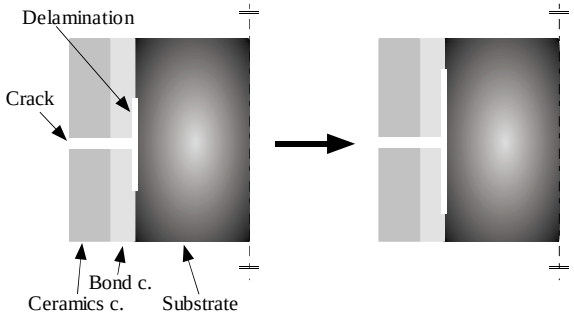

Fig.10 Damage process of the coating in pattern (C).

3.4 Large scale delamination initiated suddenly at the last stage of a fatigue test, pattern (D)

The relationship between nominal stress and surface strain under a high stress range condition at R.T. for a Z-2 specimen is shown in **Fig.11**. The surface strain gradually increased with increasing the number of cycles before a surface crack initiation, and the strain suddenly dropped to zero immediately after the crack initiation.

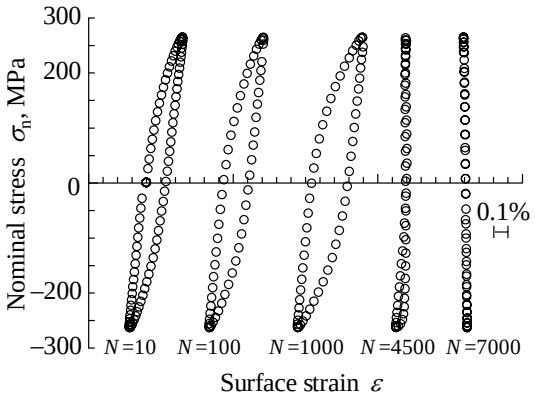

Fig.11 Stress-strain hysteresis loops under $\Delta\sigma_n$=530MPa at R.T. for a Z-2 specimen (N_f=10000).

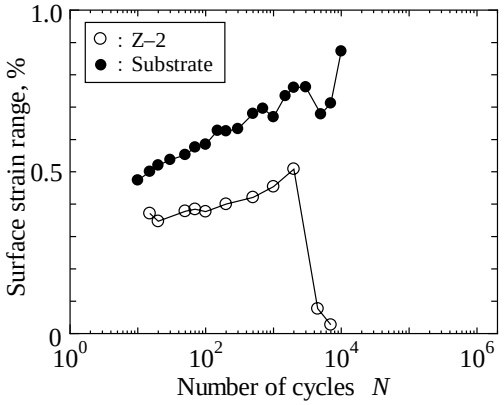

Fig.12 Comparison of the strain behavior of a Z-2 specimen and that of a substrate specimen under $\Delta\sigma_n$=530MPa at R.T.

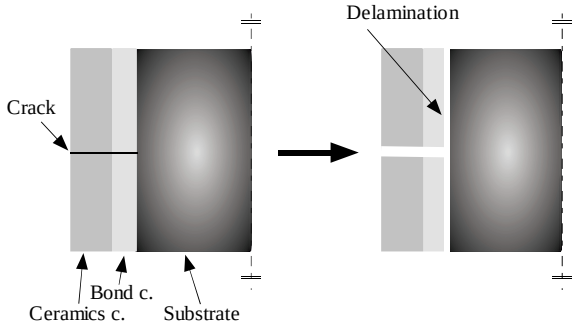

Fig.13 Damage process of the coating in pattern (D).

The comparison of the surface strain range of the Z-2 specimen and that of a substrate specimen is shown in **Fig.12**. The substrate strain appears more than 0.65% after the surface strain drops to zero as shown in Fig.12. The subsurface delamination between a substrate and a bond coating whose size was more than 5 mm distance from a surface crack was detected by the observation of the longitudinal section of the Z-2 specimen after the fatigue test. The damage process of the coating is illustrated in **Fig.13**. A surface strain was found to suddenly drop to zero when a large delamination was initiated. This strain behavior with a large delamination is called pattern (D).

3.5 Large scale delamination initiated immediately after an initial loading, pattern (E)

The relationship between nominal stress and surface strain under a high stress range condition at high temperature for an A-1 specimen is shown in **Fig.14**. The comparison of the surface strain range of the A-1 specimen and that of a substrate specimen is shown in **Fig.15**. The surface strain disappears throughout the fatigue test as shown in Fig.14 and Fig.15, though the substrate strain appeared more than 0.5%. The subsurface delamination between a substrate and a bond coating whose size was more than 5 mm distance from a surface crack was detected by the observation of the longitudinal section of the A-1 specimen immediately after loading. The damage model of the coating is illustrated in **Fig.16**. A surface strain was found to disappear throughout a fatigue test when a large delamination was initiated immediately after loading. This strain behavior with a large delamination initiated immediately after loading is called pattern (E).

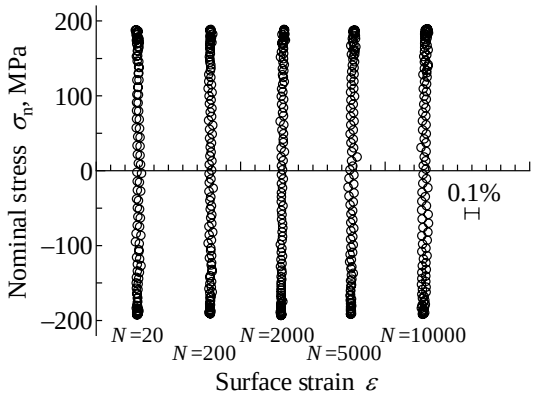

Fig.14 Stress-strain hysteresis loops under $\Delta\sigma_n$=380MPa at 893K for an A-1 specimen (N_f=11600).

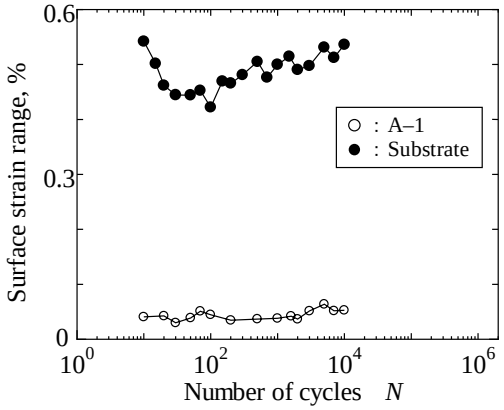

Fig.15 Comparison of the strain behavior of a A-1 specimen and that of a substrate specimen under $\Delta\sigma_n$=380MPa at 893K.

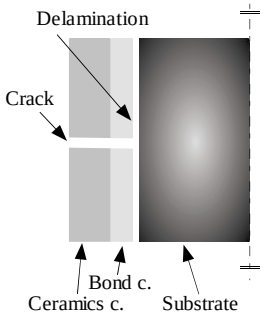

Fig.16 Damage of the coating in pattern (E).

3.6 Classification of delamination patterns

The measured damage patterns of each specimen are compared. The delaminations in A-1, Z-1 and Z-2 specimens were initiated between a bond-coating and a substrate, while the delamination in a Z-3 specimen was initiated between a ceramic-coating and a bond-coating without the delamination between a bond-coating and a substrate. Therefore, the bond-coating delamination strength of a Z-3 specimen was found to be larger than those of other specimens. Damage patterns of A-1, Z-1 and Z-2 specimens are related to both the maximum strain of the substrate and the testing temperature, and they are shown in **Figs.17(a)-(c)**. The delamination is significant in alphabetical order in Fig.17. The delamination of an A-1 specimen is more significant at high temperature than at R.T. when these are compared under the same strain range condition, and it is also significant under a high strain condition at high temperature as shown in Fig.17(a). Comparing the delamination patterns among APS bond coated specimens, the delamination damage of an A-1 specimen is more significant than that of a Z-1 specimen as shown in Figs.17(a) and (b). As the delamination between a bond-coating and a substrate of a Z-3 specimen wasn't initiated, the bond-coating delamination strength of a thermally treated specimen was found to be higher than that of a non-thermally treated specimen.

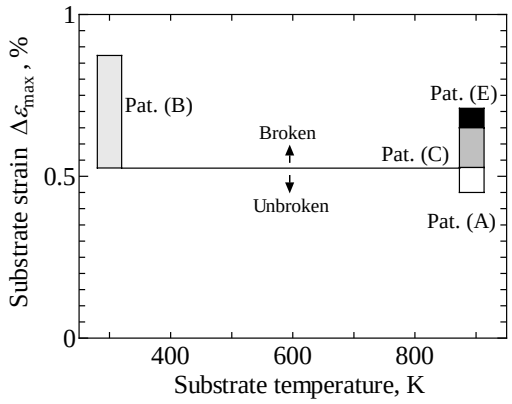

(a) A-1 specimen

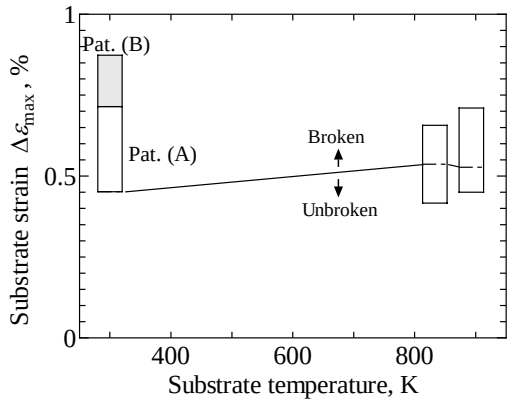

(b) Z-1 specimen

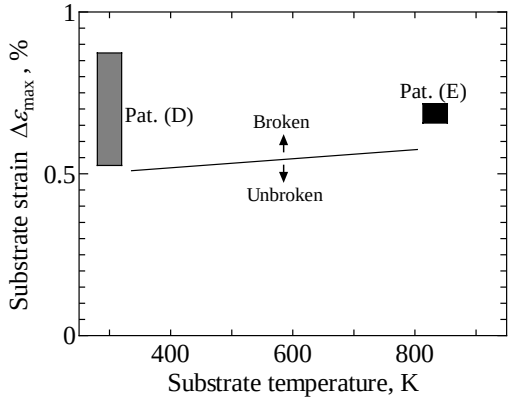

(c) Z-2 specimen

Fig.17 Coating damage patterns of each specimen.

4. Conclusions

Fatigue tests were carried out at high temperature and room temperature for ZrO_2-$8Y_2O_3$-sprayed and Al_2O_3-sprayed type 304 stainless steel specimens. Surface strain behavior during the fatigue test was measured using the laser speckle strain gauge. The relationship between the state of subsurface delamination and surface strain behavior was investigated. The results obtained are summarized as follows:

(1) The surface strain beside a crack was sensitive to the subsurface damage and applicable for evaluating the subsurface damage.
(2) It was found that surface strain was fully reflected by substrate strain unless subsurface delamination was initiated, while surface strain was found to decrease when subsurface delamination was initiated.
(3) All the surface strain behaviors were classified in five patterns, and the surface strain behaviors were related to subsurface delamination.

References

1) A. Nitta, *Journal of Society of Material Science, Japan*, **56-1**(2007), pp.90-96(in Japanese).
2) H. Waki, M. Nishii, K. Ogura and I. Nishikawa; *Trans. of the Japan Society of Mechanical Engineers A*, **66-648**(2000), pp.1520-1525(in Japanese).
3) H. Waki, K. Ogura, I. Nishikawa, H. Naganuma and M. Nishii; *Trans. of the Japan Society of Mechanical Engineers A*, **67-659**(2001), pp.1148-1154(in Japanese).
4) R. Wang and M. Kido; *J. of Nondestructive Evaluation*, **21-4**(2002), pp.117-126.
5) I. Nishikawa, K. Ogura, M. Yamagami and K. Kuwayama; *Journal of Society of Material Science, Japan*, **43-493**(1994), pp.1290-1296(in Japanese).
6) H. Waki, K. Ogura and I. Nishikawa; *JSME International Journal, Series A*, **44-3**(2001), pp.374-382.
7) H. Waki, K. Ogura, I. Nishikawa and A. Ohmori, *Materials Science and Engineering A*, **374**(2004), p 129-136.
8) E.F. Rejda, D.F. Socie and B. Beardsley; Fatigue Fract. Engng. Mater. Struct., **20**(1997), pp.1043-1050.
9) D.F. Rejda, D.F. Socie, T. Itoh, *Surface and Coatings Technology*, **113**(1999), pp.218-226.